

Original Research Article

Response surface methodology: photodegradation of methyl orange by CuO/ZnO under UV light irradiation

Siti Nur Surhayani Jefri^a, Abdul Halim Abdullah^{a,b,*}, Ernee Noryana Mohammad^a

^a Department of Chemistry, Faculty of Science, Universiti Putra Malaysia, 43400 UPM Serdang, Selangor, Malaysia

^b Institute of Advanced Technology, Universiti Putra Malaysia, 43400 UPM Serdang, Selangor, Malaysia

ARTICLE INFORMATION

Received: 28 June 2018

Received in revised: 4 October 2018

Accepted: 4 October 2018

Available online: 14 November 2018

DOI: [10.22034/ajgc.2018.135387.1078](https://doi.org/10.22034/ajgc.2018.135387.1078)

KEYWORDS

Photodegradation

ZnO doped CuO

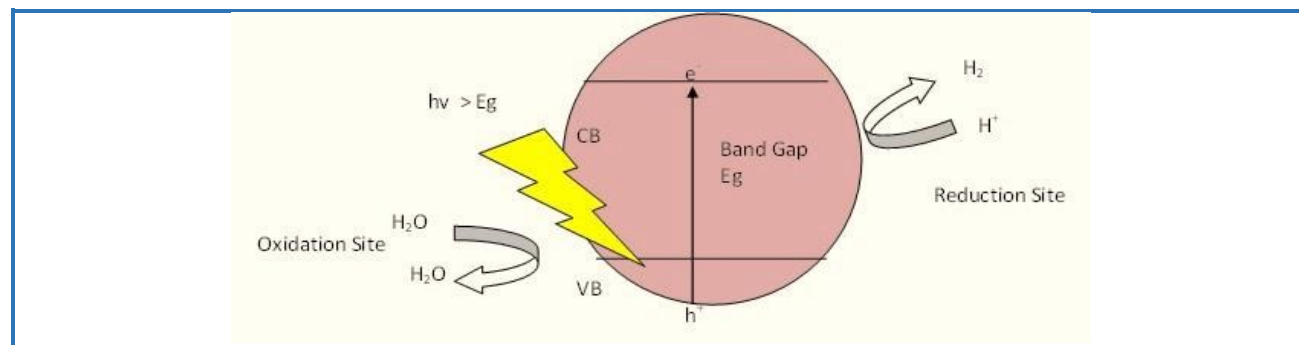
Methyl orange

UV light

ABSTRACT

Zinc oxide (ZnO) and copper oxide doped zinc oxide photocatalysts (CuO/ZnO) were synthesized by a precipitation method. The effect of CuO loading on the physicochemical properties and photocatalytic performance of ZnO in photodegrading methyl orange dye solution (MO) was investigated. The produced ZnO has a crystallite size of 61.1 nm, surface area of 4.43 nm²/g and band gap energy of 3.30 eV. After doping with 0.8% CuO, the crystallite size decreased to 19.4 nm while the surface area increased to 8.2 mm²/g. The band gap energy, however, remained the same indicating that low CuO content did not affect the optical properties of ZnO. The efficiency of the photocatalysts in photodegrading MO was evaluated under different conditions. Photocatalytic activities showed that the highest removal of 54.1% was achieved when 5 ppm of MO solution was degraded by 0.6 g of 0.8% CuO/ZnO at pH 6.8. The response surface methodology (RSM) was employed to develop a quadratic model as a functional relationship between the amounts of the degraded MO (mg/g) and three experimental factors (mass loading, MO initial concentration and MO initial pH). The highest amount of the degraded MO was 12.8 mg/g when 0.2 g of 0.8% CuO doped ZnO was used in 5 ppm MO at pH 5.

Graphical Abstract



Introduction

Methyl orange (MO) is one of the acidic dyes that is widely utilized in textile, printing, paper, food and pharmaceutical industries and research laboratories [1]. Due to its mutagenic properties, it is very important to remove the MO from these industrial wastewater [1, 2]. However, the dyes are difficult to be degraded because of their stability towards light and oxidation [2].

As a result, various techniques are employed to remove the dye elements from water such as physical, chemical and biological methods [2, 3]. But, those methods which are expensive require post-treatment of the materials or solid wastes [4]. Semiconductor photocatalytic oxidation technology has been introduced as an alternative method to remove the pollutant. TiO_2 and ZnO are the most widely used photocatalysts due to their physical and chemical stability, non-toxic, and low cost [5]. One of the major advantages of ZnO over TiO_2 is its ability to absorb greater portion of the solar light. Moreover, it is also able to remove many of the organic pollutants under visible light irradiation [6]. The irradiation of light onto the surface of the photocatalysts, with energy higher than the band gap energy, will produce electron hole pairs. These photogenerated charges, through a series of reactions, would produce radicals responsible for the degradation of the organic pollutants.

However, the rapid recombination of the photogenerated electron hole pairs, during the photocatalytic process, limits the photocatalytic efficiency of ZnO. Several researchers have reported that the photocatalytic activity of ZnO can be enhanced by being coupled with other semiconductors [7, 8], metals and metal oxides [9–12].

In this study, we aimed at improving the photocatalytic activity of ZnO by doping it with copper oxide (CuO). The ZnO/CuO photocatalysts were prepared by precipitation method. The effect of various CuO content on the physicochemical and photocatalytic properties of ZnO was investigated. The photocatalytic performance of the ZnO/CuO photocatalysts was evaluated by photodegradation of methyl orange under UV light irradiation.

Experimental

Materials and methods

The ZnO doped CuO catalyst was prepared by a co-precipitation method. A solution mixture was prepared by dissolving a fixed amount of $\text{Zn}(\text{NO}_3)_2 \cdot 6\text{H}_2\text{O}$ (Hamburg) and various amounts of $\text{Cu}(\text{NO}_3)_2 \cdot 3\text{H}_2\text{O}$ (Acros), in 100 mL of deionised water (Table 1). The solution was then titrated with 1M NaOH until pH 10 is reached and stirred for 2 h at a constant rate. The precipitate was collected by centrifugation at 3500 rpm for 10 min, and, then, was thoroughly rinsed with deionised water

before drying in oven at 70-80 °C for 24 hours. The resulting powder was grinded and calcined at 400 °C for 3 hours. Similar procedures were also used to produce the undoped ZnO.

Characterization

The crystallinity and purity of the photocatalysts were examined by X-ray diffraction (XRD, Shimadzu X-Ray with Cu radiation, $K=1.5406 \text{ \AA}$) at 40 kV, 30 mA. The XRD pattern was recorded at 2θ range of 20–60°. The surface morphology of the particles was observed by field emission scanning electron microscope (JEOL JSM-6400) and transmission electron microscope (TEM, Hitachi H-1700). The surface area and porosity measurement of the particles were determined using Quantachrome autosorb 1 controlled by Quantachrome AS 1 win software. Diffuse reflectance spectra were recorded on Shimadzu UV-3600 spectrophotometer and were used for determining the band gap of the samples.

Photodegradation of methyl orange

The photoactivity experiments were conducted by irradiating a 1000 mL MO solution containing a certain amount of suspended catalysts to the 6 watts Hitachi UV lamp (Figure 1). Air was bubbled into the reaction mixture by an air pump to ensure continuous supply of oxygen. The mixture was stirred constantly at 200 rpm to ensure a complete suspension of the catalyst. Accordingly, the experiment was performed in dark condition in order to evaluate the adsorption of MO on the catalyst. After an hour, the UV light was switched on and at regular time intervals, 10 mL of aliquots was taken throughout the 4 hours of irradiation time and, then, filtered using cellulose 0.45 μm membrane filter. The residual concentration of the MO was then measured using PerkinElmer Lambda 35 UV-Vis spectrophotometer. All the photocatalytic degradation experiments were carried out in triplicate. The percentage degradation and amount of MO degraded were calculated using equation 1 and 2, respectively:

$$\text{Photodegradation (\%)} = ((C_0 - C_t) / C_0) \times 100\% \quad (1)$$

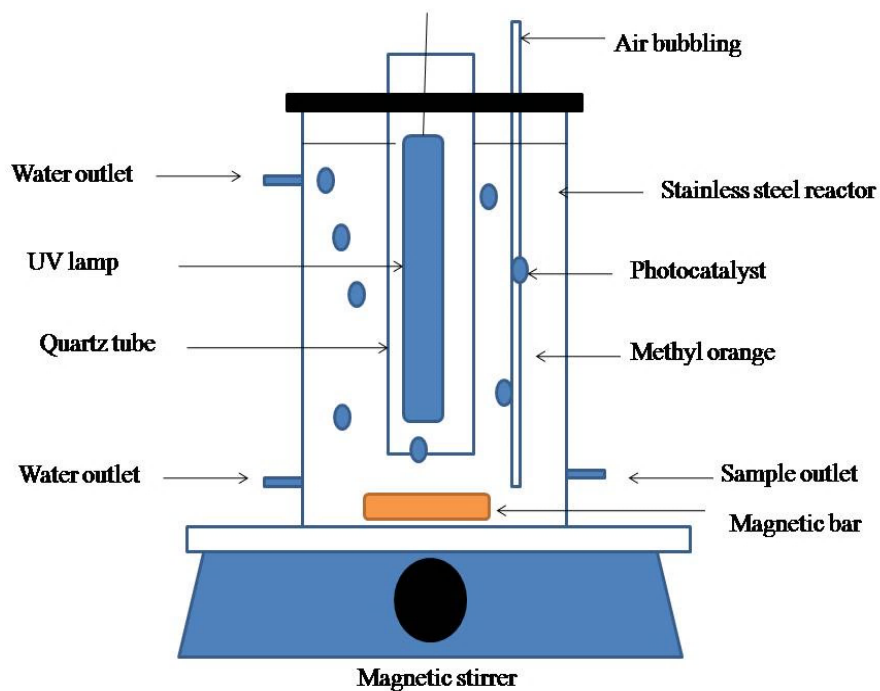
$$\text{Amount of MO degraded (mg/g)} = ((C_0 - C_t) / m) \times V \quad (2)$$

Where C_0 and C_t is the concentration of MO initially and at time t , respectively, m is the mass of photocatalyst and V is the volume of MO solution.

Response surface methodology (RSM)

Table 1. The composition of the solution mixture for the preparation of ZnO and CuO doped ZnO photocatalysts

Catalysts	Weight of $\text{Zn}(\text{NO}_3)_2 \cdot 6\text{H}_2\text{O}$ (g)	Weight of $\text{Cu}(\text{NO}_3)_2 \cdot 3\text{H}_2\text{O}$ (g)
ZnO		0
0.2% CuO/ZnO		0.0242
0.4% CuO/ZnO		0.0483
0.6% CuO/ZnO	14.8735	0.0725
0.8% CuO/ZnO		0.0967
1.0% CuO/ZnO		0.1208

**Figure 1.** Schematic diagram of the photoreactor

Response surface methodology (RSM) was used to optimize the reaction conditions of the MO photodegradation. Three variables namely ZnO/CuO mass loading, the initial concentration and initial pH of MO solution were chosen as the independent variable while the amount of MO removal (mg/g) was set as the output response variable. The ranges and levels of the variables are as shown in Table 2. Design expert V.7.1.5 software was used for the response surface modelling, statistical analysis and optimization. The combination effect of the three variables was investigated using

central composite design (CCD). 20 sets of experiments including six replications were performed (Table 3). The data were analyzed using the analysis of variance (ANOVA) and, also, the optimal value of the MO removal was estimated using the 3D response surface analysis of the variables.

Results and discussion

Screening experiments

In order to determine the most suitable photocatalyst to be used in this study, the performance of the prepared CuO/ZnO photocatalysts was evaluated and compared to that of ZnO. Figure 2 showed that the performance of 0.2% CuO/ZnO catalyst was comparable to that of the pure ZnO. The photocatalytic performance of the CuO/ZnO catalysts increased with increasing CuO loading up to 0.8%. The increase in photocatalytic activity of the catalyst can be attributed to the increase in the surface area of the catalyst. As the surface area increased, more light can be absorbed by the photocatalysts leading to a generation of higher amount of the radical species responsible for the degradation of the MO dye. At the highest CuO loading (1%), the photodegradation activity decreased. This could be due to the reduction in the surface area of the photocatalysts. In addition, CuO at higher loading could act as the recombination sites which increase the electron hole recombination rate leading to a decrease in the photocatalytic activity of the catalyst [13]. Based on the screening experiments, 0.8% CuO/ZnO exhibited the highest photocatalytic activity which was accordingly used in further experiments.

Characterization of the photocatalysts

Figure 3 shows the XRD pattern of ZnO and CuO/ZnO photocatalysts. The XRD peaks observed for the photocatalysts are characteristics of ZnO with hexagonal structure. No peak associated with CuO was observed due to its small content in the photocatalyst. Despite their similar XRD patterns, both of the photocatalysts matched a different JCPDS file (Table 4), indicating that the addition of CuO onto ZnO has a slight effect on the structure of ZnO. The intensity of the peaks also decreased with increasing CuO content. The crystallite size of the prepared catalysts (Table 4), estimated by the use of Debye Scherrer equation, decreased with increasing CuO content up to 0.8% but then increased. The lattice parameter of the undoped ZnO also decreased slightly upon the addition of CuO. This may indicate that CuO has been successfully doped into ZnO. The decreasing crystallite size might be due to the incorporation of CuO into the structure *via* substitution of Zn^{2+} by Cu^{2+} . This could eventually change the crystal growth kinetics of the CuO/ZnO photocatalysts, thus resulting in the formation of structure with smaller lattice parameter [14, 15].

Table 2. Variables and their coded levels and actual values

Variable	Range and Level		
	Low	Medium	High
pH	5	8	11
Mass Loading (g)	0.2	0.6	1.0
Initial Concentration (ppm)	5	17.5	30

Table 3. Design layout of central composite design (CCD) for removal of MO with experimental and predicted responses

Run Order	Independent Variables			Removal(mg/g)	
	A = pH	B= Mass of Catalyst (g)	C= MO Concentration (ppm)	Predicted	Actual
1	5	0.2	5.0	13.1	12.75
2	11	0.6	17.5	5.1	4.97
3	11	0.2	5.0	11.4	11.78
4	5	0.6	17.5	6.9	7.13
5	8	0.6	30.0	3.1	3.8
6	5	1.0	5.0	2.1	2.76
7	11	1.0	5.0	0.9	0.92
8	8	1.0	17.5	6.7	6.06
9	11	0.2	30.0	0.64	0
10	5	0.2	30.0	3.0	3.0
11	8	0.6	17.5	7.01	7.43
12	8	0.6	17.5	7.01	6.83
13	11	1.0	30.0	4.5	4.92
14	5	1.0	30.0	6.4	6
15	8	0.6	17.5	7.01	6.85
16	8	0.6	17.5	7.01	7.09
17	8	0.6	5.0	6.4	5.78
18	8	0.2	17.5	10.3	11.01
19	8	0.6	17.5	7.01	6.42
20	8	0.6	17.5	7.01	7.32

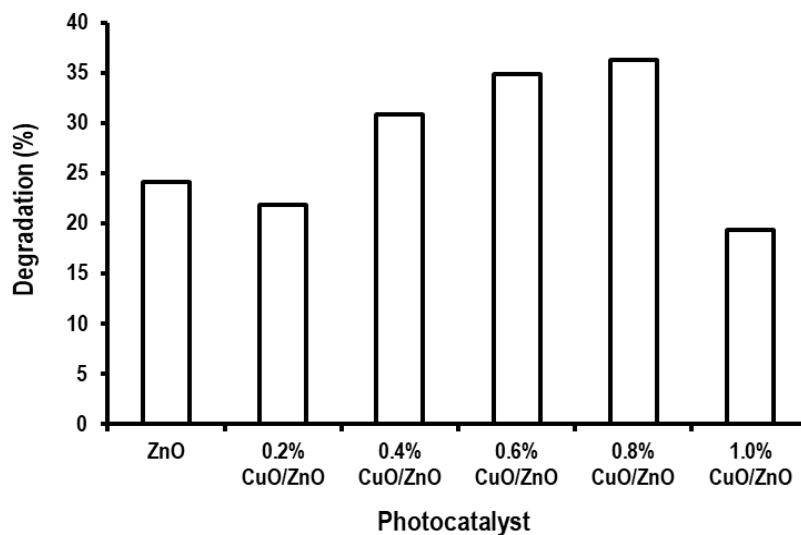


Figure 2. Photodegradation of methyl orange by ZnO and CuO/ZnO photocatalysts. Condition: mass of catalyst = 0.20 g, MO concentration = 10 ppm, pH = 6.8)

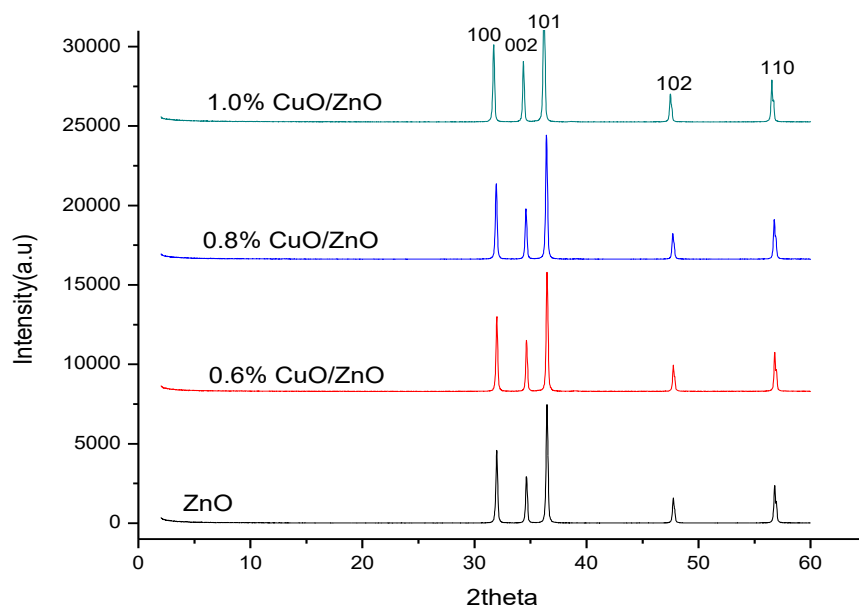


Figure 3. XRD diffractometer for ZnO and CuO/ZnO prepared with different percentage of CuO

The morphology of the photocatalysts was recorded using FESEM and TEM. As illustrated in [Figure 4](#), the pure ZnO exhibited irregular shape [Figure 4a](#) which then changed to rod shape upon the addition of CuO ([Figure 4b, C and d](#)). This clearly showed that the addition of CuO affects the growth and eventually the morphology of ZnO [13]. The particles were densely agglomerated at the highest CuO content (1%).

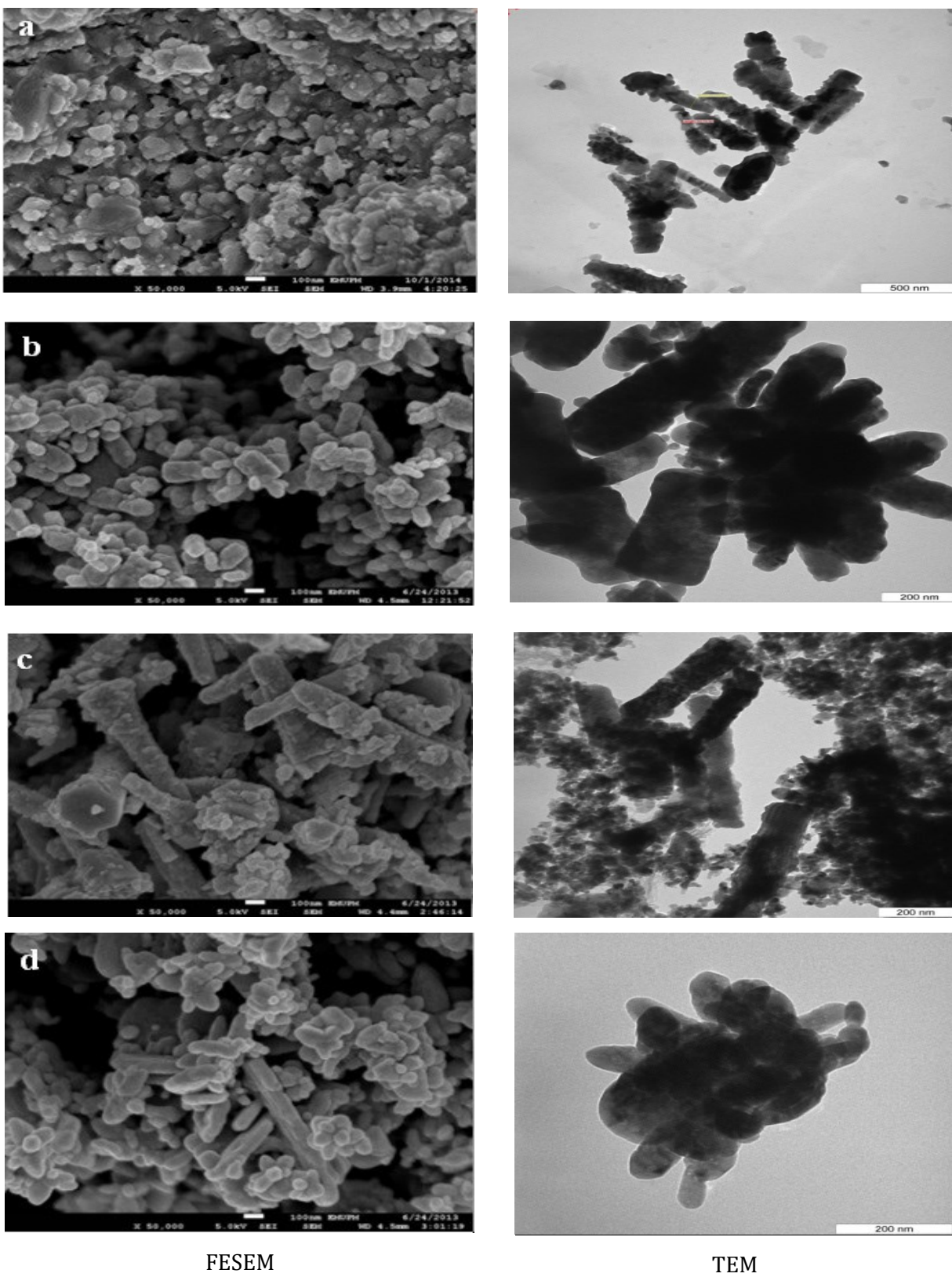


Figure 4. The FESEM and TEM images of a) ZnO, b) 0.6% ZnO/CuO, c) 0.8% ZnO/CuO and d) 1.0% ZnO/CuO

The surface area and the band gap energy for ZnO and CuO/ZnO photocatalysts are shown in Table 4. The surface area of the photocatalyst increases as the percentage of CuO is increased up to 0.8%. This can be attributed to the influence of CuO on particle aggregation which, by its involvement in the nucleation and growth of ZnO, may result in doping-induced lattice deformation and formation of oxygen vacancies [16]. The decreased in the surface area of 1% CuO/ZnO might be due to the deposition of excess crystalline CuO on the surface of ZnO [13]. Therefore, the highest photoactivity observed for 0.8% CuO/ZnO in the screening experiment can be attributed to its small particle size and high surface area.

The band gap energy of photocatalysts was calculated using the following equation 3:

$$E_g = h(c/\lambda) \quad (3)$$

where, h is the Planck's constant, c is the speed of light, and λ is the wavelength. The λ values were obtained from the intercept of the R% vs wavelength plot (Figure 5). As shown in Table 4, the calculated band gap energy of ZnO and CuO/ZnO photocatalysts was exactly the same indicating the addition of low CuO content into ZnO did not influence the optical properties of the ZnO.

Effect of catalyst loading

The effect of catalyst loading was studied by varying the mass of 0.8% CuO/ZnO catalyst from 0.2 to 1.0 g in the photodegradation of 10 ppm MO. Table 5 showed that the percentage degradation of MO increased with increasing mass loading is up to the 0.6 g.

before it decreased at 0.8 g. The experimental data was also fitted to the Langmuir Hinshelwood kinetic model and the plot of $\ln C/C_0$ vs time (Figure 6) showed that the photodegradation of MO followed the pseudo-first-order reaction. The apparent rate constants, k_{app} , were determined from the slope of the plot and are shown in Table 5.

As the mass of catalyst increased up to 0.6 g, more hydroxyl and superoxide radicals are generated. Since the concentration of the MO is fixed at 10 ppm, the ratio of the available MO dyes molecules to the generated hydroxyl and superoxide radicals is low [17]. The rate of MO photodegradation also increased from $9 \times 10^{-4} \text{ min}^{-1}$ to $1.2 \times 10^{-3} \text{ min}^{-1}$, thus higher percentage of MO degradation was observed. At higher catalyst loading (0.8 g and above), the rate of MO photodegradation decreased to $7 \times 10^{-4} \text{ min}^{-1}$ which consequently led to a decrease in the percentage of MO degradation. This is might be due to aggregation of the photocatalyst which could cause a decrease in the surface area available for the photodegradation to take place. At the same time, the reaction mixture became more turbid and cloudy. Due to light scattering effect, less amount of light

can be absorbed by the photocatalyst which eventually reduced the photogenerated radicals thus the efficiency of the photodegradation process [18, 19].

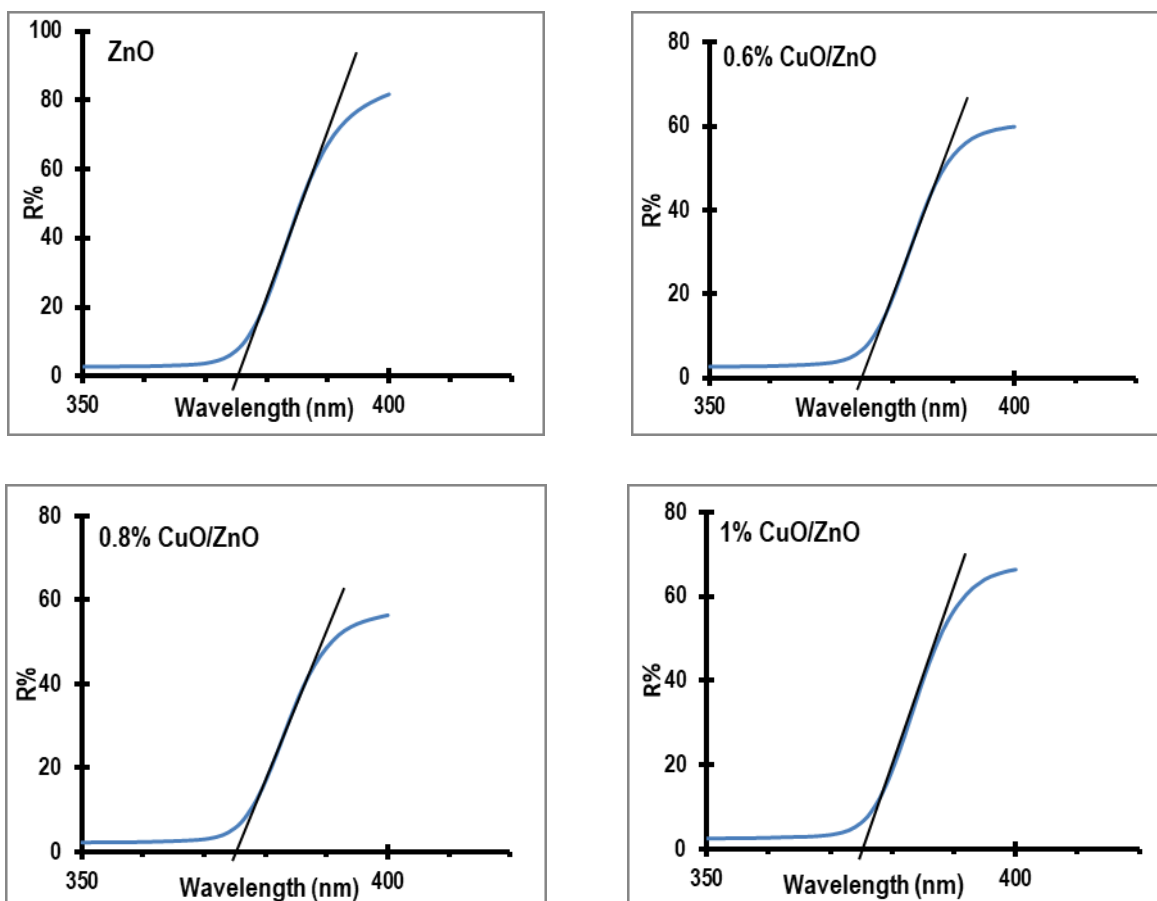


Figure 5. Diffuse reflectance UV-Vis spectra for ZnO and CuO/ZnO photocatalysts

Effect of pH

In order to study the effect of pH on the MO photodegradation process, the initial pH of the solution (pH 6.8) was adjusted to the desired pH using 1.0 M HCl and 1.0 M NaOH. As shown in [Figure 7](#), the percentage degradation of MO increased with increasing pH and reached optimum at pH 6.8 but then decreased at pH 8.

The photocatalytic activity of metal oxides can be affected by their acid–base behavior [20] and the surface charge of the photocatalyst as the surface of the photocatalyst can be protonated or deprotonated by the solution at different pH [21]. Although the surface of the photocatalyst is positively charged in acidic condition, low percentage of MO photodegradation was observed at pH 5 and this could be attributed to the dissolution of the photocatalyst particle under mild acidic condition [22, 23]. As the pH of the solution is increased to 6.8, more MO anions attracted to the

positively charged surface of the catalyst, hence the degradation of MO became more efficient. In basic condition, deprotonation of the surface may occur producing a negatively charged surface. Consequently, there exist a stronger repulsion between the MO anions and the surface of the photocatalyst resulting in the decrease of MO photodegradation.

Effect of MO concentration

The effect of the initial concentration of methyl orange, ranging from 5 to 30 ppm, on the photodegradation efficiency was investigated and the result is illustrated in [Figure 8](#). The result shows that the percentage of MO degradation decreased with the increasing MO concentration. Since the irradiation time and the mass of photocatalyst were kept constant, the hydroxyl radical produced on the photocatalyst surface was also constant. As the concentration of the MO increases, the ratio of free radicals (Hydroxyl and superoxide) to the dye molecules decreases, hence lesser amount of MO dye molecules were degraded.

The decrease in the percentage degradation can also be attributed to the screening effect of the MO dye molecules. Based on Beer–Lambert law, as the initial concentration of dyes increases, the path length of photons penetrating the solution decreases and the photons will be intercepted before reaching the surface of photocatalyst. Consequently, reducing the photon absorption on the photocatalyst surfaces [19]. In addition, the adsorption of MO dye on the surface of the photocatalyst can also increase at higher MO concentration. Both phenomenon reduces the generation of the free radicals hence reduces the efficiency of the photocatalyst to degrade the MO dye molecules.

Response surface methodology

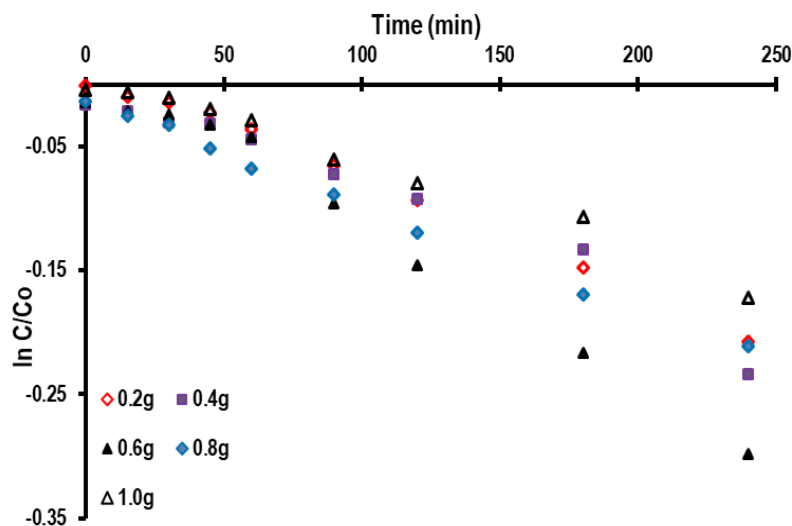
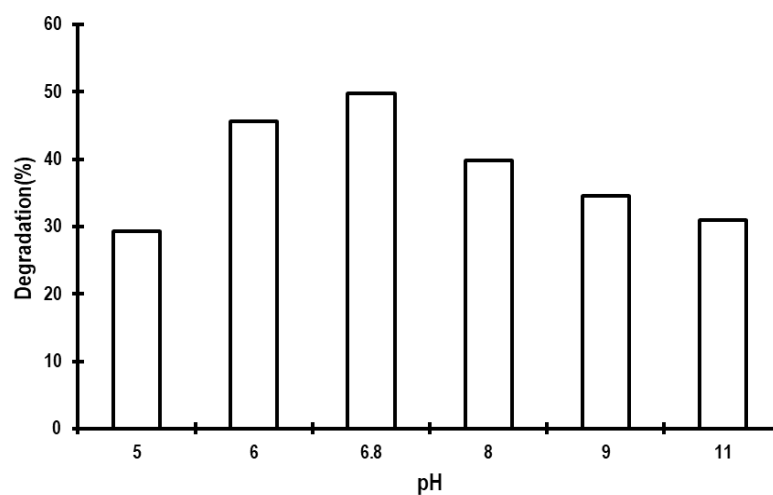
To optimize the photodegradation of MO, CCD was used and multiple polynomial regression analysis was performed with resulting data. The experimental and predicted responses are shown in [Table 3](#). The regression analysis for the MO removal fitted the quadratic model and is expressed by the second order polynomial equation 4.

$$y = 7.01 - 0.90A - 1.79B - 1.63C + 0.13AB - 0.16AC + 3.60BC - 0.99A^2 - 1.50B^2 - 2.25C^2 \quad (4)$$

where y is the predicted amount of MO removed (mg/g) while A, B, and C are the coded values of the independent variables.

Table 4. Physical properties of ZnO and CuO/ZnO photocatalysts

Catalyst	JCPDS File Number	Crystallite Size (nm)	Lattice Parameter (Å)			Surface Area (m ² /g)	Band gap (eV)
			a	b	c		
ZnO	01-080-0074	61.0	3.253	3.253	5.215	4.43	3.30
0.6% CuO/ZnO	00-065-3411	32.9	3.249	3.249	5.207	5.21	3.30
0.8% CuO/ZnO	00-065-3411	19.4	3.249	3.249	5.207	8.22	3.30
1.0% CuO/ZnO	00-065-3411	47.5	3.249	3.249	5.207	5.22	3.30

Figure 6. Kinetics of MO photodegradation at various amount of 0.8% CuO/ZnO catalyst (Conditions: 10 ppm MO; pH 6.8)**Figure 7.** Photodegradation of MO by CuO/ZnO photocatalyst at various pH of the solution (Conditions: 0.6 g of photocatalyst, 10 ppm of MO)

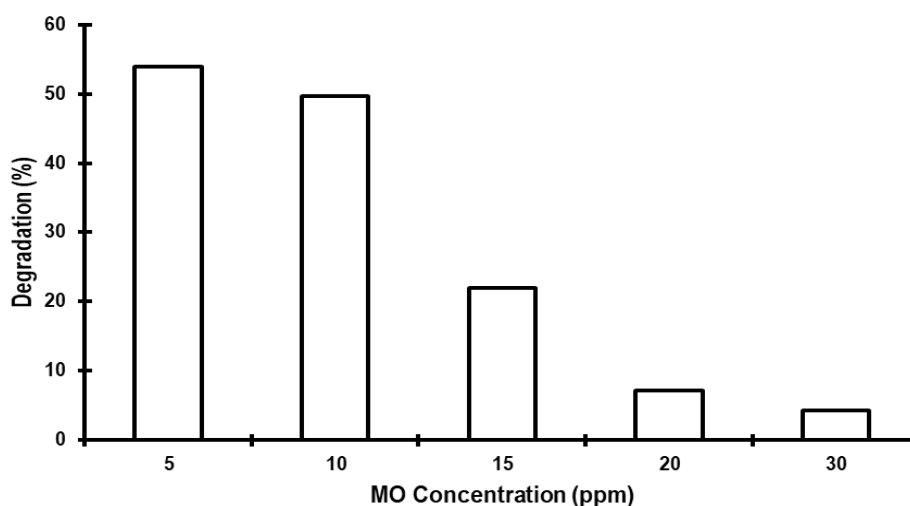


Figure 8. Photodegradation of MO of various concentrations by CuO/ZnO photocatalyst (Conditions: 0.6 g of photocatalyst, pH 6.8)

Table 5. Photodegradation of MO using various amount of 0.8% CuO/ZnO catalyst (Conditions: 10 ppm of MO at pH 6.8)

Mass Loading (g)	MO degradation (%)	Apparent Rate Constant, k_{app} ($\times 10^{-3} \text{ min}^{-1}$)	Correlation factor (R^2)
0.2	36.3	0.9	0.992
0.4	37.2	0.9	0.954
0.6	49.7	1.2	0.980
0.8	34.8	0.8	0.996
1	31.8	0.7	0.981

The P-value of the main effects, A, B, and C, on the removal of MO is significant (Table 6). The interaction term for BC and the quadratic term for A^2 , B^2 and C^2 also contribute significantly to the removal of MO as their P-values are less than 0.05. The analysis of variance (ANOVA) was utilized to test the significance of each term in the equation and to fit the obtained regression model (Table 7). The F-value of the model of 54.89 implies the model is significant with 0.01% chance that this could be due to noise. The F-value of lack of fit of 4.52 is not significant as its P-value is above 0.05. The coefficient of the determination shows the model is significant with $R^2 = 0.980$ while the adjusted $R^2 = 0.962$. The regression model demonstrates a better relationship between independent variables and the response.

The effects of the independent variables and combined effects of each independent variable on the response variable were illustrated by 3D response surface plots. [Figure 9a](#) presented the effect of the mass loading of photocatalyst and the pH of the MO solution. The amount of MO degraded decreased with increasing mass of the photocatalyst regardless of the pH of the MO solution which could be attributed to the agglomeration of the photocatalyst and light scattering effect. The amount of MO degraded however remained almost constant when the pH of the solution is increased to 6 but then decreased with increasing pH. It was observed that the amount of MO degraded is greater at low catalyst loading and in acidic condition.

[Figure 9b](#) showed the effect of initial concentration and initial pH of MO solution while the mass loading of the CuO/ZnO is kept at central level. The plot shows the amount of MO degraded decreased at both high concentration and high pH of the MO solution. This is attributed to the light screening effect of MO and strong repulsion between the MO anion and the negatively charged surface of the catalyst.

Table 6. Estimated regression coefficient of independent variables for MO removal

Factor	Coefficient Estimate	Standard Error	P-value
Intercept	7.01	0.22	-
A	-0.90	0.20	0.0011
B	-1.79	0.20	<0.0001
C	-1.63	0.20	<0.0001
AB	0.13	0.22	0.5688
AC	-0.16	0.22	0.4923
BC	3.60	0.22	<0.0001
A ²	-0.99	0.38	0.0264
B ²	1.50	0.38	0.0028
C ²	-2.25	0.38	0.0001

Notes: Coefficient of Determination, $R^2 = 0.980$, R^2 (adjusted) = 0.962. Abbreviation: df, degree of freedom

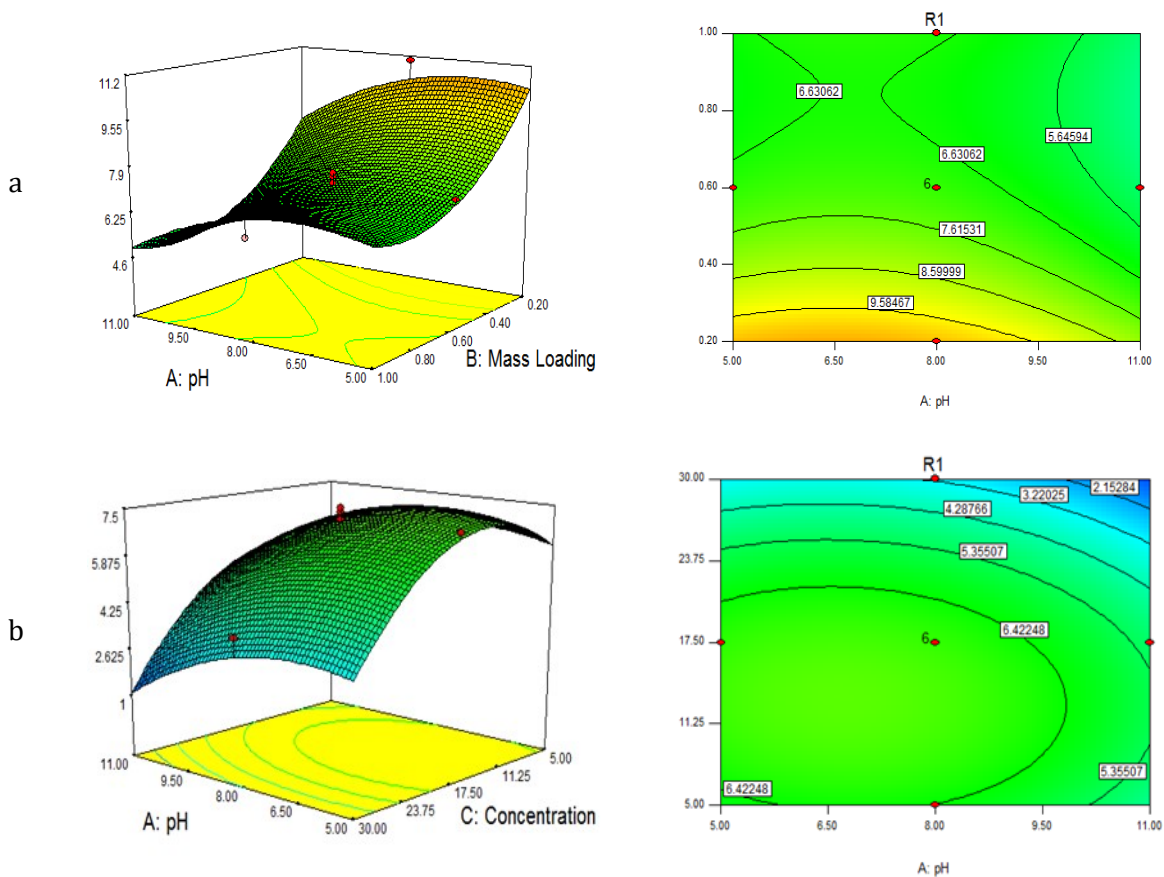
The effect of MO concentration and catalyst loading is depicted in [Figure 9c](#). The amount of MO degraded decreased with increasing MO concentration and catalyst loading. This indicate that the photodegradation process is efficient at low MO concentration and catalyst loading as the solution allows more UV light penetration leading to activation of more active catalytic sites, hence resulting in a higher amount of MO degraded.

Model validation

The developed model predicted that the highest amount of MO degraded (13.16 mg/g) can be achieved at optimum conditions of 0.2 g 0.8% CuO/ZnO photocatalyst, 5 ppm of MO concentration and pH 5. An experiment was performed at the predicted optimized conditions in order to validate the model. The result showed that 12.75 mg/g of MO can be degraded which was in good agreement with the predicted value. This can be confirmed that response surface methodology can be used to optimize the photodegradation of methyl orange.

Table 7. Anova for the MO removal

Source	Sum of Squares	df	Mean Square	F-value	P-value
Model	196.07	9	21.795	54.89	<0.0001
Residual	3.97	10	0.4	-	-
Lack of Fit	3.25	5	0.65	4.52	0.0617
Pure Error	0.72	5	0.14	-	-
Cor Total	200.04	19	-	-	-



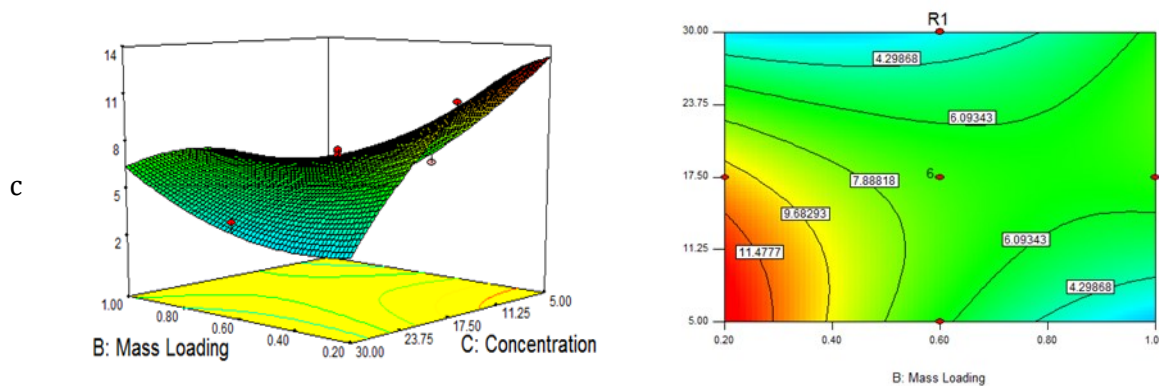


Figure 9. Three dimensional response surface plots showing the effect between a) Ph of MO solution and catalyst loading, b) pH and concentration of the MO solution and c) catalyst loading and concentration of MO degraded

Conclusion

The efficiency of ZnO in photodegradation of methyl orange is enhanced by addition CuO. The highest percentage of MO photodegradation of 54.1% was achieved when 0.6 g of 0.8% CuO/ZnO photocatalyst was used to degrade 5 ppm of MO solution at pH 6.8. The enhanced efficiency could be attributed to the morphology and surface area of the photocatalyst.

Disclosure statement

No potential conflict of interest was reported by the authors.

References

- [1]. Mittal A., Malviya A., Kaur D., Mittal J., Kurup L. *J. Hazard. Mater.*, 2007, **148**:229
- [2]. Chen S., Zhang J., Zhang C., Yue Q., Li Y., Li C. *Desalination*, 2010, **252**:149
- [3]. Crini G. *Bioresour. Technol.*, 2006, **97**:1061
- [4]. Pérez M.H., Peñuela G., Maldonado M.I., Malato O., Fernández-Ibáñez P., Oller I., Gernjak W., Malato S. *Appl.Catal. B: Environ.*, 2006, **64**:272
- [5]. Wojtoniszak M., Zielinska B., Chen X., Kalenczuk R.J., Borowiak-Palen E. *J. Mater. Sci.*, 2012, **47**:3185
- [6]. Shinde D.R., Tambade P.S., Chaskar M.G., Gadave K.M. *Drink. Water Eng. Sci.*, 2017, **10**:109
- [7]. Cheng C., Amini A., Zhu C., Xu Z., Song H., Wang N. *Sci. Rep.*, 2014, **4**:4181
- [8]. Apostolescu G.A., Cernatescu C., Cobzaru C., Tataru-farmus R.E., Apostolescu N. *Environ. Eng. Manag. J.*, 2015, **14**:415
- [9]. Bouzid H., Faisal M., Harraz F.A., Al-Sayari S.A., Ismail A.A. *Catal. Today*, 2015, **252**:20

- [10]. Ahmad M., Ahmed E., Zhang Y., Khalid N.R., Xu J., Ullah M., Hong Z. *Curr. Appl. Phys.*, 2013, **13**:15
- [11]. Ali A.M., Ismail A.A., Najmy R., Al-Hajry A. *J. Photochem. Photobiol. A. Chem.*, 2014, **275**:37
- [12]. Balachandran S., Swaminathan M. *J. Phys. Chem. C*, 2012, **116**:26306
- [13]. Saravanan R., Karthikeyan S., Gupta V.K., Narayanan V., Stephen A. *Mater. Sci. Eng. C.*, 2013, **33**:91
- [14]. Gopinathan E., Viruthagiri G., Shanmugam N., Sathiya-priya S. *Optik*, 2015, **126**:5830
- [15]. Chang Y.C., Lin P.S., Liu F.K., Guo J.Y., Chen C.M. *J. Alloys Compd.*, 2016, **688**:242
- [16]. Fu C., Gong Y., Wu Y., Liu J., Zhang Z., Li C., Niu L. *Appl. Surf. Sci.*, 2016, **379**:83
- [17]. Abdullah A.H., Moey H.J.M., Yusof N.A., *J. Environ. Sci.*, 2012, **24**:1694
- [18]. Akyol A., Yatmaz H.C., Bayramoglu M. *Appl. Catal. B: Environ.*, 2004, **54**:19
- [19]. Chakrabarti S., Dutta B.K. *J. Hazard. Mater.*, 2004, **112**:269
- [20]. Sakthivel S., Neppolian B., Shankar M.V., Arabindoo B., Palanichamy M., Murugesan V. *Sol. Ene. Mater. Sol. Cells*, 2003, **77**:65
- [21]. Elangovan S.V., Chandramohan V., Sivakumar N., Senthil T.S. *Superlatt. Microst.*, 2015, **85**:901
- [22]. Achouri F., Corbel S., Balan L., Mozet K., Girot E., Medjahdi G., Said M.B., Ghrabi A., Schneider R. *Mater. Des.*, 2016, **101**:309
- [23]. Ashar A., Iqbal M., Bhatti I.A., Ahmad M.Z., Qureshi K., Nisar J., Bukhari I.H. *J. Alloys Compd.*, 2016, **678**:126

How to cite this manuscript: Siti Nur Surhayani Jefri, Abdul Halim Abdullah*, Ernee Noryana Mohammad. Response surface methodology: photodegradation of methyl orange by CuO/ZnO under UV light irradiation. *Asian Journal of Green Chemistry*, 3(2) 2019, 271-287 DOI: [10.22034/ajgc.2018.135387.1078](https://doi.org/10.22034/ajgc.2018.135387.1078)